Ultra-broadband optical parametric generation in periodically poled stoichiometric $LiTaO_3$

Martin Levenius,* Valdas Pasiskevicius, Fredrik Laurell, and Katia Gallo

KTH – Royal Institute of Technology, Department of Applied Physics,
Roslagstullsbacken 21, SE-106 91 Stockholm, Sweden
**ml@laserphysics.kth.se*

Abstract: We report on broadband gain in an optical parametric generator based on periodically poled 1 mol% magnesium-doped stoichiometric $LiTaO_3$ (PPMg:SLT). More than an octave-spanning parametric gain, stretching from near to mid-infrared, is generated by pumping the crystals close to the point where, at parametric degeneracy, the waves experience zero group-velocity dispersion. Using a picosecond Ti:sapphire source, we measured the broadest parametric gain bandwidths, 180 THz at 10 dB, in PPMg:SLT gratings with a period of 25 μm pumped at 860 nm.

OCIS codes: (190.4410) Nonlinear optics, parametric processes; (190.4400) Nonlinear optics, materials; (190.7110) Ultrafast nonlinear optics.

References and links

1. E. Sorokin, S. Naumov, and I. T. Sorokina, "Ultrabroadband infrared solid-state lasers," IEEE J. Sel. Top. Quantum Electron. **11**(3), 690–712 (2005).
2. J. M. Dudley, G. Genty, and S. Coen, "Supercontinuum generation in photonic crystal fiber," Rev. Mod. Phys. **78**(4), 1135–1184 (2006).
3. C. Manzoni, G. Cirmi, D. Brida, S. De Silvestri, and G. Cerullo, "Optical-parametric-generation process driven by femtosecond pulses: Timing and carrier-envelope phase properties," Phys. Rev. A **79**(3), 033818 (2009).
4. L. E. Myers, G. D. Miller, R. C. Eckardt, M. M. Fejer, R. L. Byer, and W. R. Bosenberg, "Quasi-phase-matched 1.064-μm-pumped optical parametric oscillator in bulk periodically poled $LiNbO_3$," Opt. Lett. **20**(1), 52–54 (1995).
5. H. Karlsson, and F. Laurell, "Electric field poling of flux grown $KTiOPO_4$," Appl. Phys. Lett. **71**(24), 3474–3476 (1997).
6. C. Heese, C. R. Phillips, L. Gallmann, M. M. Fejer, and U. Keller, "Ultrabroadband, highly flexible amplifier for ultrashort midinfrared laser pulses based on aperiodically poled Mg:$LiNbO_3$," Opt. Lett. **35**(14), 2340–2342 (2010).
7. G. Cerullo, and S. De Silvestri, "Ultrafast optical parametric amplifiers," Rev. Sci. Instrum. **74**(1), 1–18 (2003).
8. P. D. Trapani, A. Andreoni, C. Solcia, P. Foggi, R. Danielius, A. Dubietis, and A. Piskarskas, "Matching of group velocities in three-wave parametric interaction with femtosecond pulses and application to traveling-wave generators," J. Opt. Soc. Am. B **12**(11), 2237–2244 (1995).
9. D. Brida, C. Manzoni, G. Cirmi, M. Marangoni, S. Bonora, P. Villoresi, S. De Silvestri, and G. Cerullo, "Few-optical-cycle pulses tunable from the visible to the mid-infrared by optical parametric amplifiers," J. Opt. **12**(1), 013001 (2010).
10. A. Gaydardzhiev, I. Nikolov, I. Buchvarov, V. Petrov, and F. Noack, "Ultrabroadband operation of a femtosecond optical parametric generator based on BiB_3O_6 in the near-IR," Opt. Express **16**(4), 2363–2373 (2008).
11. P. S. Kuo, K. L. Vodopyanov, M. M. Fejer, D. M. Simanovskii, X. Yu, J. S. Harris, D. Bliss, and D. Weyburne, "Optical parametric generation of a mid-infrared continuum in orientation-patterned GaAs," Opt. Lett. **31**(1), 71–73 (2006).
12. M. Tiihonen, V. Pasiskevicius, A. Fragemann, C. Canalias, and F. Laurell, "Ultrabroad gain in an optical parametric generator with periodically poled $KTiOPO_4$," Appl. Phys. B **85**(1), 73–77 (2006).
13. O. Prakash, H. H. Lim, B. J. Kim, K. Pandiyan, M. Cha, and B. Rhee, "Collinear broadband optical parametric generation in periodically poled lithium niobate crystals by group velocity matching," Appl. Phys. B **92**(4), 535–541 (2008).
14. S. V. Tovstonog, S. Kurimura, and K. Kitamura, "High power continuous-wave green light generation by quasiphase matching in Mg stoichiometric lithium tantalate," Appl. Phys. Lett. **90**(5), 051115 (2007).
15. N. E. Yu, S. Kurimura, Y. Nomura, M. Nakamura, K. Kitamura, Y. Takada, J. Sakuma, and T. Sumiyoshi, "Efficient optical parametric oscillation based on periodically poled 1.0 mol % MgO-doped stoichiometric $LiTaO_3$," Appl. Phys. Lett. **85**(22), 5134–5136 (2004).

#140056 - $15.00 USD Received 22 Dec 2010; revised 8 Feb 2011; accepted 8 Feb 2011; published 16 Feb 2011

16. F. Rotermund, C. Yoon, V. Petrov, F. Noack, S. Kurimura, N.-E. Yu, and K. Kitamura, "Application of periodically poled stoichiometric $LiTaO_3$ for efficient optical parametric chirped pulse amplification at 1 kHz," Opt. Express **12**(26), 6421–6427 (2004).
17. F. Rotermund, V. Petrov, E. Noack, V. Pasiskevicius, J. Hellstrom, F. Laurell, H. Hundertmark, P. Adel, and C. Fallnich, "Compact all-diode-pumped femtosecond laser source based on chirped pulse optical parametric amplification in periodically poled $KTiOPO_4$," Electron. Lett. **38**(12), 561–563 (2002).
18. G. Marcus, A. Zigler, D. Eger, A. Bruner, and A. Englander, "Generation of a high-energy ultrawideband chirped source in periodically poled $LiTaO_3$," J. Opt. Soc. Am. B **22**(3), 620–622 (2005).
19. V. Pasiskevicius, and F. Laurell, "Optical parametric generators and amplifiers," in *Mid-Infrared Coherent Sources, NATO Science Series*, M. Ebrahimzadeh, and I. Sorokina, eds. (Springer, 2008).
20. V. Z. Kolev, M. W. Duering, and B. Luther-Davies, "Corrections to refractive index data of stoichiometric lithium tantalate in the 5-6 microm range," Opt. Lett. **31**(13), 2033–2035 (2006).
21. I. P. Kaminow, and W. D. Johnston, "Quantitative Determination of Sources of the Electro-Optic Effect in $LiNbO_3$ and $LiTaO_3$," Phys. Rev. **160**(3), 519–522 (1967).
22. J. F. Pinto, L. Esterowitz, and G. H. Rosenblatt, "Frequency tripling of a Q-switched Cr:LiSAF laser to the UV region," IEEE J. Sel. Top. Quantum Electron. **1**(1), 58–61 (1995).

1. Introduction

Access to broadband coherent gain in the spectral regions of near to mid-infrared is essential for a variety of applications requiring broadly tunable and/or ultrashort optical pulses, such as ultrafast imaging, time-resolved spectroscopy, remote sensing or metrology. Mode-locked Cr^{2+}:ZnSe or Cr^{2+}:ZnS lasers can provide short mid-infrared pulses, which nevertheless are ultimately limited by the gain bandwidths of such crystals, stretching from approximately 2 to 3 μm [1]. Supercontinuum fibre sources represent an appealing possibility for broadband generation, due to high modal confinement and the capability to engineer the group velocity dispersion (GVD) [2], but offer limited control over the spectral coherence and power scalability of the output radiation.

On the other hand, parametric frequency down-conversion in quadratic nonlinear media provides a high-coherence approach, suitable for the generation and amplification of broad bandwidths of intense radiation, which can also be compressed to yield extremely short pulse durations [3]. The reduced thermal load of parametric processes is also an advantage when targeting high power operation. The efficiency and wavelength flexibility of quasi-phase matched (QPM) materials such as periodically poled $LiNbO_3$ (PPLN) or $KTiOPO_4$ (PPKTP) [4,5] are particularly appealing for optical parametric generation (OPG) and amplification (OPA). QPM allows the use of the largest component of the nonlinear susceptibility tensor and overcomes dispersion constraints to phase matching, enabling to choose freely the working points within the transparency range of the substrate. The technique also allows non-critical phase matching, permitting parametric interactions to be implemented in collinear geometries. Moreover, further enhancements in device wavelength tunability (albeit at the expense of a reduction in efficiency) can be afforded through super-structured QPM grating designs, as recently demonstrated for aperiodically poled gratings in $LiNbO_3$, where OPA bandwidths of the order of 1 μm in the mid-IR have been achieved [6].

Nevertheless, QPM in itself does not ensure the group-velocity matching (GVM) of quadratic non-degenerate three-wave mixing processes, which on the other hand is an essential prerequisite in order to achieve bandwidths suitable for ultra-short pulse generation or amplification. Several approaches have been demonstrated to address the issue of GVM in OPG and OPA devices. The difference in group velocity between the signal and idler waves can be compensated by adopting non-collinear interaction geometries [7], which, however suffer from the limitations to the device length (hence the efficiency) imposed by pulse spatial walk-off. Furthermore, non-collinear schemes have the drawback of inducing a pulse-front tilt of the output beam and an output direction that can vary with broad tuning ranges [8]. An alternative approach, allowing collinear interactions, involves choosing a spectral location for OPG in proximity of the zero group velocity dispersion (GVD) point of the material, where signal and idler group velocities are truly matched for a range of wavelengths, as has recently been suggested [9]. This grants, in principle, access to the broadest bandwidths. The approach has been demonstrated by exploiting birefringent phase matching [10], but can be readily

#140056 - $15.00 USD Received 22 Dec 2010; revised 8 Feb 2011; accepted 8 Feb 2011; published 16 Feb 2011

implemented in QPM materials thanks to the freedom in determining the OPG spectral working points through a suitable choice of the grating period.

The first demonstration of broadband down-conversion close to the point of zero GVD in a QPM medium was achieved with orientation-patterned GaAs, which displayed a 20 dB OPG bandwidth of 39 THz when pumped around 3.3 μm [11]. Periodically poled KTP, $LiNbO_3$ and $LiTaO_3$ can offer alternative QPM solutions, enabling operation with pump wavelengths in the near infrared. 10 dB bandwidths of ~150 THz and ~100 THz have been demonstrated for OPG in PPKTP and PPLN, pumped at 830 and 930 nm, respectively [12,13]. Nevertheless, KTP conversion bandwidths are limited on the long-wavelength side by the absorption edge of the material (~3.5 μm). Such a limitation does not apply to $LiNbO_3$ and $LiTaO_3$ substrates, given their broader transparency range (extending beyond 4 μm). On the other hand, these crystals can suffer from effects such as photorefraction or green-induced infrared absorption, which can compromise their performance at the high powers that are often desired in conjunction with broad bandwidths, e.g. in optical chirped pulse amplification (OPCPA) systems [7].

In recent years, new crystal growth techniques have been devised to produce $LiNbO_3$ and $LiTaO_3$ crystals of modified compositions (nearly stoichiometric and Mg-doped) in order to overcome the limitations associated with the relatively low optical damage thresholds and elevated poling fields of standard congruent $LiNbO_3$ and $LiTaO_3$. Among the modified crystals, 1 mol% magnesium-doped stoichiometric $LiTaO_3$ (Mg:SLT) has demonstrated exceptionally good power-handling capabilities even for room-temperature operation, made possible by its reduced photorefraction and low thermo-optic coefficients [14]. The low coercive field of Mg:SLT, which is somewhat below that of KTP and one order of magnitude lower than that of $LiNbO_3$, also permits up-scaling of device apertures to millimetre sizes [15]. Recent results in periodically poled Mg:SLT (PPMg:SLT) [16] proved a performance comparable to that of PPKTP for high gain single stage OPCPA, for ultra-short pulses near 1.57 μm [17]. Somewhat larger spectral extents (~40 THz) have been attained for Ti:sapphire-pumped OPG in PPSLT, yet with a working point still far away from zero GVD [18].

In this paper we demonstrate ultra-broadband OPG in periodically poled Mg:SLT, achieved through GVM in the vicinity of the point of zero GVD. The broadest OPG spectrum in our experiments span a 10 dB bandwidth of 180 THz (stretching from below 1.2 μm to above 3.5 μm) which, to the best of our knowledge, represents the highest value reported for collinear parametric down-conversion to date. The measured spectra exhibit also a remarkable flatness, which makes them particularly well-suited for perspective applications to ultra-short pulse generation and amplification.

2. Collinear broadband OPG condition

The parametric gain of an OPG or OPA process depends on the wave vector mismatch Δk, the length of the nonlinear crystal L, the nonlinear coefficient d_{eff}, the pump intensity I_{p}, the interacting wavelengths λ_x (x = p, pump; s, signal; i, idler) and the corresponding indices of refraction n_x. In the case of a strong, undepleted, pump the gain takes the following form [19]:

$$G = \Gamma^2 \frac{\sinh^2\left(L\sqrt{\Gamma^2 - \left(\frac{\Delta k}{2}\right)^2}\right)}{\Gamma^2 - \left(\frac{\Delta k}{2}\right)^2}, \qquad \Gamma^2 = \frac{8\pi^2 d_{\mathrm{eff}}^2 I_{\mathrm{p}}}{n_{\mathrm{p}} n_{\mathrm{s}} n_{\mathrm{i}} \lambda_{\mathrm{s}} \lambda_{\mathrm{i}} \varepsilon_0 c}. \tag{1}$$

With reference to the experimental conditions described in the next section, we shall restrict our analysis to collinear interactions, quasi-phase matched via a uniform grating of period Λ.

#140056 - $15.00 USD Received 22 Dec 2010; revised 8 Feb 2011; accepted 8 Feb 2011; published 16 Feb 2011

Accordingly, the phase mismatch in Eq. (1) will be given by: $\Delta k = k_p - k_s - k_i - 2\pi/\Lambda$, $k_x = n_x\omega_x/c$ being the wave propagation constants for the interacting frequencies ω_x (x = p,i,s).

The OPG gain bandwidth is maximised when, for a fixed pump frequency ω_p, the variation of the phase mismatch with respect to the signal frequency is minimised. Using a Taylor series expansion around the QPM point ω_0 (where $\Delta k \equiv 0$), the phase mismatch can be expressed as a function of the signal deviation ($\Delta\omega = \omega_s - \omega_0$) as follows:

$$\Delta k(\Delta\omega) = \left[\frac{1}{v_s} - \frac{1}{v_i}\right]\Delta\omega + \frac{1}{2}\left[\beta_{2s} + \beta_{2i}\right](\Delta\omega)^2 + O(\Delta\omega)^3, \qquad (2)$$

where $v_{s,i} = (\partial k/\partial\omega)^{-1}_{s,i}$ are the group velocities and $\beta_{2s,i} = (\partial^2 k/\partial\omega^2)_{s,i}$ the GVD coefficients of signal and idler, calculated at the QPM working point ($\omega_s = \omega_0$, $\omega_i = \omega_p - \omega_0$). The broadest bandwidth is attained by letting the wavelength of degeneracy for signal and idler approach the point of zero GVD of the material, which in the case of Mg:SLT is estimated to lie at $\lambda_{s,i}$ ~1820 nm (i.e. λ_p ~910 nm), after the Sellmeier equations available from literature on SLT [20].

Knowing the zero-GVD point of the substrate, one can then in principle identify the QPM grating period required to access the broadband OPG region. Nevertheless, the actual optimum working point in the experiments may differ from theoretical predictions, which become extremely sensitive to uncertainties in the Sellmeier equations in the vicinity of zero GVD. Moreover, pumping an OPG process exactly at half the zero-GVD wavelength might not necessarily correspond to the optimum for achieving the broadest bandwidths, because of the effect of higher order terms in the expansion of Eq. (2), as seen in PPKTP experiments [12]. Therefore in view of investigating broadband OPG in PPMg:SLT we set up to map a broader parameter range in the spectral region around the expected zero GVD point, using multiple poling periods, namely Λ = 25, 26 and 27 μm.

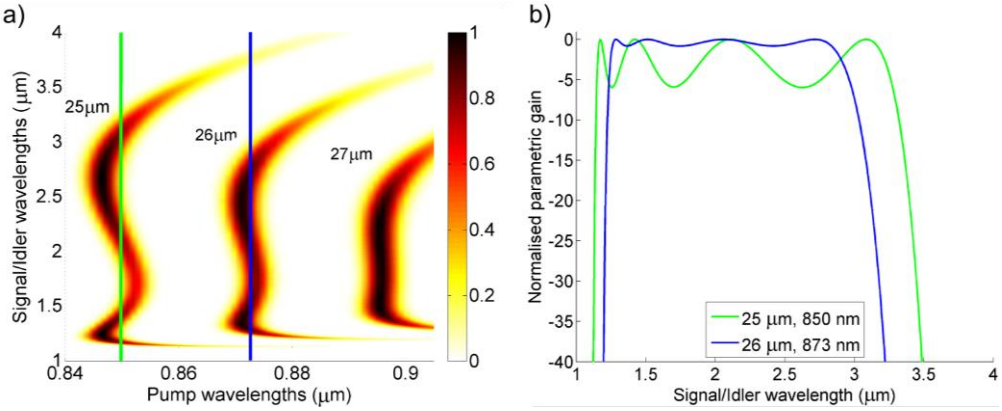

Fig. 1. Normalised gain for broadband OPG in PPSLT at T = 80°C, pumped with I_p = 10 GW/cm^2. Calculations based on Eq. (1) and Sellmeier equations for SLT [20]. a). Contour plots of the gain as a function of pump and signal/idler wavelengths for QPM periods Λ = 25, 26 and 27 μm. b) OPG spectra corresponding to the working points indicated by the two vertical lines in the diagrams of Fig. 1a. Green line: Λ = 25 μm and λ_p = 850 nm; blue line: Λ = 26 μm and λ_p = 873 nm.

Figure 1a shows the contour plots of the normalised parametric gain for the three PPMg:SLT periods we chose for our OPG experiments. The curves are calculated from Eq. (1) using the Sellmeier equations for SLT [20]. The expected OPG spectral distributions at two specific working points on the QPM diagram of Fig. 1a (at λ_p = 850 nm for Λ = 25 μm and at λ_p = 873 nm for Λ = 26 μm, marked by the green and blue lines, respectively) are illustrated by the curves of Fig. 1b.

#140056 - $15.00 USD Received 22 Dec 2010; revised 8 Feb 2011; accepted 8 Feb 2011; published 16 Feb 2011

3. Experiments

For the experiments we fabricated multi-grating QPM structures by conventional electric-field poling performed on commercially available z-cut, 0.5 mm-thick, 1 mol% Mg:SLT crystals (Oxide Corp.). The poling was performed at room temperature by applying electrical pulses close to the coercive field (E_c ~1.2 kV/mm) via periodic electrodes, defined through lithographic patterning of photoresist followed by the deposition of a thin metal layer on the +*z* face of the ferroelectric substrates. The resulting domain patterns faithfully reproduced the electrode mask, consisting of three 2-mm-wide bands with periods of 25, 26 and 27 μm, with good uniformity over the whole device length (1 cm).

To characterise the PPSLT response in down-conversion we employed a tunable picosecond Ti:sapphire amplifier system (Fig. 2). A Nd:YVO_4 pumped femtosecond source seeded a regenerative chirped pulse amplifier delivering micro-joule pulses at 1 kHz with bandwidths of $\Delta\lambda_p \approx 2$ nm. The OPG response for all three grating periods was examined with pump wavelengths (λ_p) ranging from 820 to 900 nm and pulse durations between 1.5 and 2.7 ps. The pump beam, polarised along the z-axis of the PPMg:SLT samples, was loosely focused inside the crystal using a 300 mm lens. The sample was kept at 80°C and mounted on a translation stage to allow full probing of the QPM bands. Throughout the experiments we ensured that the pump wave vector and the QPM grating vector in the sample were collinear.

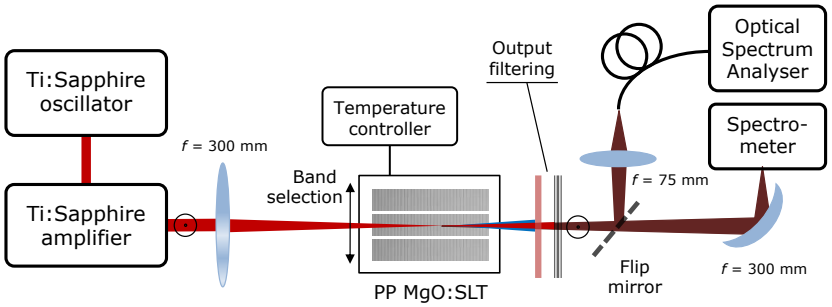

Fig. 2. Sketch of the setup used for the OPG experiments. The OPG pump was a Ti:sapphire amplified laser system delivering μJ-pulses, with picosecond durations at 1 kHz. The input beam was loosely focused by a 300 mm lens into the PPMg:SLT crystals, heated to 80°C. The OPG output was fibre-coupled to an optical spectrum analyser. Spectral measurements extending beyond 1.75 μm were performed with a free-space coupled spectrometer.

At the crystal output a dichroic mirror rejected most of the pump beam. Additionally, we inserted an OG570 glass filter to remove the light up-converted in the PPMg:SLT crystals by cascaded sum-frequency generation processes (see next section). The optical output of the crystals was then focused into a fibre-coupled optical spectrum analyser (OSA), Ando AQ6315A, sensitive up to 1750 nm, to routinely perform spectral measurements on the OPG signals. To extend the characterisation to the full OPG response from the near to the mid-infrared we alternatively free-space coupled the PPMg:SLT output into a spectrometer; a scanning Horiba Jobin Yvon monochromator (iHR550) equipped with a PbSe detector head which, used with a lock-in amplifier, was sensitive up to 4.8 μm.

4. Results and discussion

Systematic spectral measurements performed in the three PPMg:SLT bands for various pump wavelengths (λ_p = 0.82 – 0.9 μm) indicated broadband OPG in both the 25 and the 26 μm grating periods. The broadest bandwidths were achieved by pumping the former at λ_p = 860 nm and the latter at λ_p = 880 nm. Figure 3 shows the measured OPG spectra, obtained with 1.5 ps pump pulses at powers of 16 and 22 mW (for Figs. 3a and 3b, respectively). In both cases the input beam was focused to a 230 μm beam radius ($1/e^2$) in the sample.

The broadest signal spectrum (Fig. 3a) spans a 3 dB bandwidth of 70 THz. It is obtained using a pump wavelength of 860 nm, which is shorter than half the wavelength for zero-GVD

#140056 - $15.00 USD Received 22 Dec 2010; revised 8 Feb 2011; accepted 8 Feb 2011; published 16 Feb 2011

(λ_p = 910 nm), as expected from the Sellmeier equations [20]. An experimental shift of the OPG optimum towards shorter wavelengths is consistent with previous observations in other materials [12]. Furthermore, uncertainties in the Sellmeier equations also contribute to the discrepancy in λ_p. When comparing the recorded spectra of Fig. 3 with the predictions of Fig. 1b, it can be noticed that, even though the exact pump wavelengths used to generate the broadest spectra differ, the spectral extent of the signals matches the predictions rather well. Thus a simple shift of the QPM curves in Fig. 1a towards longer pump wavelengths would provide a reasonably good agreement with the experimental results. As mentioned in Section 2, an offset between theory and experiments can reasonably be expected to occur for the optimum OPG wavelengths due to an increased sensitivity of the predictions to errors in the Sellmeier equations in the spectral region close to the zero-GVD point.

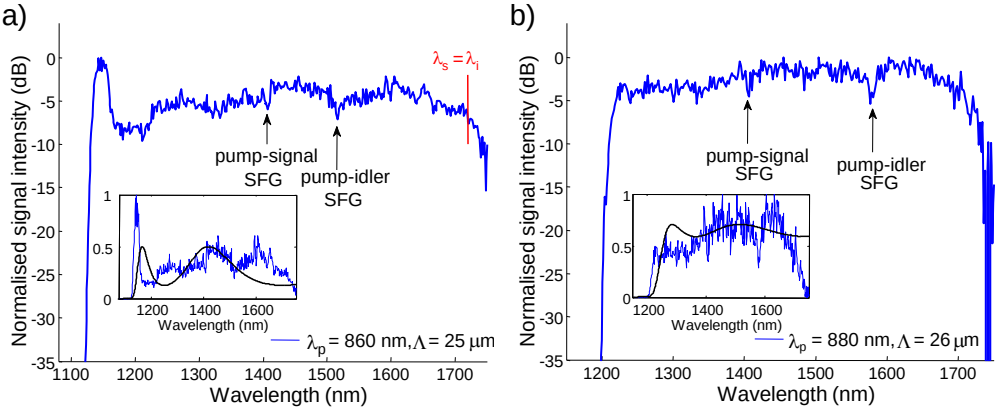

Fig. 3. OPG signal spectra from 1 mol% PPMg:SLT at T = 80°C. a) Spectral response measured from the 25 μm QPM band for a pump of 860 nm, with a pulse energy of 16 μJ generating 30 nJ OPG pulses. The integration time of the OSA was 1 ms and the spectrum was the average over 5 measurements. The inset shows the same spectrum in linear scale (blue curve), with the theoretical prediction of Fig. 1b added (black curve). b) Same as a), this time for the 26 μm band, with a 22 μJ pump at 880 nm, generating 40 nJ OPG pulses. In both cases the input beam consisted of Gaussian pulses with a duration of 1.5 ps, focused to a beam radius of 230 μm in the sample.

Further comparison of the experimental results and the predicted spectra (Figs. 3 and 1b, respectively), discloses differences in the internal structure of the OPG signal band. Such deviations are to be attributed to the fact that the theoretical spectra are calculated for a strictly monochromatic pump, whereas the pump in the experiment has a spectral extent of 2 nm. Thus the experimentally generated output represents a weighted sum of spectra of the type shown in Fig. 1b, obtained at neighbouring pump wavelengths. As a result, the modulations seen in the predicted spectrum smear out in the experiments, yielding an OPG band with less structure. The spectral extent of the pump can also explain the more pronounced peak appearing at 1150 nm in Fig. 3a. Here the pump covers at the same time a part of the vertical region of the 25 μm QPM curve (Fig. 1a), responsible for the broadband conversion, and a section of the lower horizontal QPM branch, where signal photons at 1150 nm are generated. The stronger inflection of the QPM curve for 25 μm, as compared to the 26 μm QPM curve, results in the peak observed in the measurements of Fig. 3a.

An additional feature of the spectra obtained in PPMg:SLT is their remarkable flatness, in contrast to reported results for broadband OPG in PPKTP and PPLN, where significant dips in the signal and idler spectrum were carved out by cascaded up-conversion processes [12,13]. There is evidence of similar processes occurring also in our experiments, yet with a much lower efficiency and thus smaller impact on the flatness of the OPG spectra. The arrows in Fig. 3 indicate spectral features in the OPG spectra which can be associated to concurrent sum frequency generation (SFG) between the pump and the generated signal, achieved through third order QPM, and SFG between the pump and the generated idler, via second order QPM.

#140056 - $15.00 USD Received 22 Dec 2010; revised 8 Feb 2011; accepted 8 Feb 2011; published 16 Feb 2011

The predicted QPM wavelengths for these processes match quite well the spectral locations of the dips seen in the spectrum of Fig. 3a, at λ_s = 1515 nm (2nd order QPM for pump-idler SFG, with Λ = 25 μm) and λ_s = 1406 nm (3rd order QPM for pump-signal SFG). Similar calculations done for Λ = 26 μm predict declines in intensity at 1580 nm and at 1405 nm, consistent with the experimental observations (Fig. 3b).

The span of the OSA measurement in Fig. 3a covers also the degeneracy wavelength, $\lambda_{s,i}$ = 1720 nm (indicated by the red mark), and it can be noticed that the intensities are not symmetric around the degeneracy point. Instead they appear to monotonically decrease on the longer wavelength side. As a matter of fact, such a decaying trend at the edge of the OSA spectral range appears to be an artefact of the instrument, as confirmed by the sets of measurements that we subsequently performed on the OPG output with the spectrometer. With the latter we could also directly measure the full OPG bandwidths, covering both the signal and idler spectral ranges.

One such measurement, corrected for the absorption of the optical elements between the PPMg:SLT sample and the detector, is shown in Fig. 4, where we plot the experimental data (solid blue curve) recorded at the same working point as the one of Fig. 3a (Λ = 25 μm, λ_p = 860 nm). From Fig. 4 it is apparent that there is no real decrease in powers beyond the degeneracy point (indicated by the red mark).

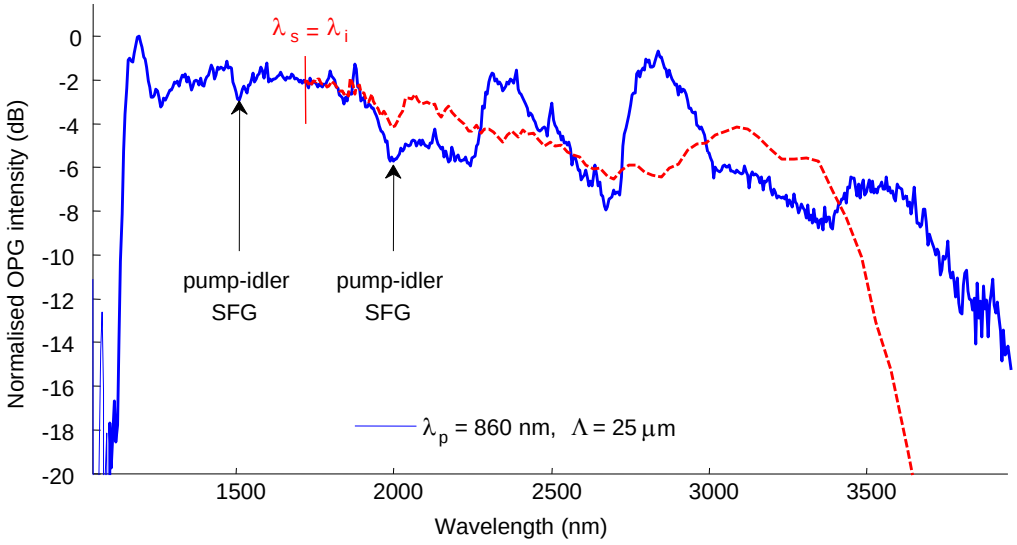

Fig. 4. Full OPG spectra from 1 mol% PPMg:SLT at T = 80°C, generated with 25 μm period using a pump beam of 860 nm, 78 mW power and 2.7 ps pulse duration focused to 100 μm radius. The dashed red line represents a prediction of the idler intensities, calculated from the detected signal intensities. The integration time of the PbSe detector used with the Horiba Jobin Yvon monochromator was 900 ms.

To distinguish the contribution of OPG from that of other parametric processes observed on the long-wavelength side of the experimental data, in Fig. 4 we plot a prediction of the idler spectrum (red dashed curve). It is calculated from the signal intensities ($\lambda_s < 2\lambda_p$) by using the Manley-Rowe relations: $P_s/\omega_s = P_i/\omega_i = -P_p/\omega_p$, where P_x and ω_x are the power and frequency, respectively, of the interacting waves.

By comparing this prediction with the measurement we can identify three features in the idler spectrum which do not seem to be arising directly from the OPG process, namely the three broad peaks located at λ_i = 2.4, 2.8, 3.5 μm. The nature of those additional contributions to the PPMg:SLT output is the subject of current investigations. Their spectral locations match fairly well the expected positions for the 6th, 5th and 4th harmonics of a polariton wave

#140056 - $15.00 USD Received 22 Dec 2010; revised 8 Feb 2011; accepted 8 Feb 2011; published 16 Feb 2011

at 20 THz [21], which would strongly support their interpretation as the outcome of a concurrent stimulated Raman scattering process occurring in the sample.

A conservative estimate for the spectral extent of OPG in Fig. 4, based on the Manley-Rowe prediction for the longer-wavelength edge of the spectrum (neglecting the even broader tail seen in the experiments), indicates a bandwidth spanning more than one octave. The bandwidth at 10 dB is 180 THz, which is, to the best of our knowledge, the broadest band achieved so far in collinear parametric down-conversion.

In the spectrum of Fig. 4 we also pointed out spectral features associated to cascaded SFG processes (already discussed with reference to the spectra in Fig. 3) occurring in the sample. The signatures of pump-idler SFG, achieved by 2nd order QPM, can be discerned among the idler wavelengths at 2 μm and at the corresponding signal wavelength of 1510 nm. On the other hand, pump-signal SFG does not seem to notably affect the spectrum.

As a final remark on the measurements of Fig. 4, the total energy content of the detected OPG pulses was 2 μJ for an input energy of 78 μJ (the threshold was ~1 μJ). The maximum fluctuations observed in the OPG output energy (monitored with a Newport germanium 918D-IR-OD3 photodetector) over a time of 5 minutes, noted for all the measurements of Figs. 3 and 4, amounted to $\Delta\mathcal{E}/\mathcal{E}$ = 7%. Preliminary measurements of the OPG response as a function of pump energy, for the conditions of Fig. 4, show that a linear regime prevails up to ~20 μJ, with a slope conversion efficiency of 6%. Saturation effects appearing at higher pump energies reduce the conversion efficiency to 3% at the highest investigated pump energy. The OPG energy can be further increased by realising an OPA scheme following the OPG stage. In addition, the low coercive field of Mg:SLT allows for thicker crystals to be periodically poled, which could enable further scaling to higher powers.

5. Conclusion

We have reported on ultra-broadband parametric gain in periodically poled Mg:SLT, pumped with picosecond pulses in the vicinity of the zero GVD point of the material. OPG bandwidths as broad as 180 THz (at 10 dB), spanning the full spectrum from 1.1 to 3.5 μm, were achieved with a pump at 860 nm in PPMg:SLT with 25 μm poling periods. This is to the best of our knowledge the broadest band observed in collinear parametric down-conversion to date. When compared to previous results in PPLN and PPKTP, OPG in PPMg:SLT exhibited also a remarkable spectral flatness.

The combination of extremely broad bandwidths and high parametric gain [16] affordable in PPMg:SLT makes this material a promising candidate for applications to high-power, ultra-short pulse generation and amplification Given the optimum pump wavelength of 860 nm, it is interesting to consider broadband parametric systems pumped by Cr:LiSAF lasers and amplifiers, which can be directly diode pumped and can also generate large pulse energies at this wavelength [22].

Acknowledgements

This work was partially supported by the Linnaeus Centre ADOPT, the Swedish Research council (Vetenskapsrådet), the Knut and Alice Wallenberg Foundation, and the EU 7th Framework Programme. K. G. Also gratefully acknowledges support from the European Commission through a Marie Curie grant (PIEF-GA-2009-234798).

#140056 - $15.00 USD Received 22 Dec 2010; revised 8 Feb 2011; accepted 8 Feb 2011; published 16 Feb 2011